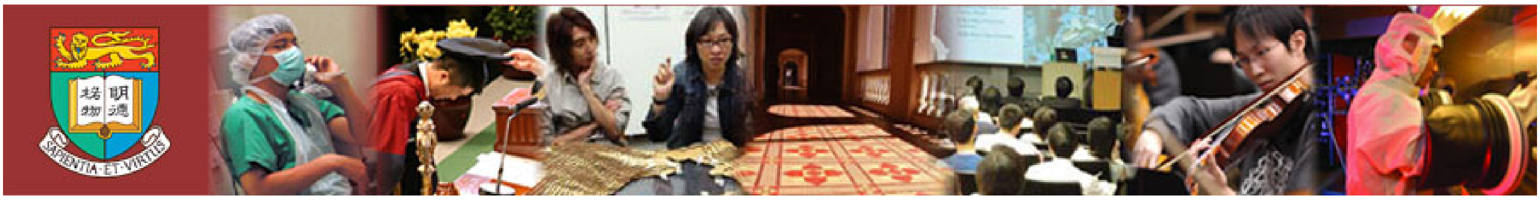

Title	Novel geometric coordination registration in cone-beam computed tomogram
Author(s)	Lam, WYH; Ngan, HYT; Wat, PYP; Luk, HWK; Pow, EHN; Goto, TK
Citation	The 2014 IEEE Applied Imagery Pattern Recognition Workshop (AIPR), Washington, DC., 14-16 October 2014. In Applied Imagery Pattern Recognition Workshop Proceedings, 2014, p. 1-6
Issued Date	2014
URL	http://hdl.handle.net/10722/214776
Rights	Applied Imagery Pattern Recognition Workshop Proceedings. Copyright © IEEE, Computer Society.

Novel Geometric Coordination Registration in Cone-beam Computed Tomogram

Walter Y.H. Lam*, Henry Y.T. Ngan†, *Senior Member, IEEE*, Peter Y.P. Wat*,
Henry W.K. Luk*, Edmond H.N. Pow*, Tazuko K. Goto*
*Faculty of Dentistry, The University of Hong Kong, Pokfulam, Hong Kong
†Department of Mathematics, Hong Kong Baptist University, Kowloon Tong, Hong Kong
Email: ehnpow@hku.hk

***Abstract*— The use of cone-beam computed tomography (CBCT) in medical field can help the clinicians to visualize the hard tissues in head and neck region via a cylindrical field of view (FOV). The images are usually presented with reconstructed three-dimensional (3D) imaging and its orthogonal (x-, y- and z- planes) images. Spatial relationship of the structures in these orthogonal views is important for diagnosis of diseases as well as planning for treatment. However, the non-standardized positioning of the object during the CBCT data acquisition often induces errors in measurement since orthogonal images cut at different planes might look similar. In order to solve the problem, this paper proposes an effective mapping from the Cartesian coordinates of a cube physically to its respective coordinates in 3D imaging. Therefore, the object (real physical domain) and the imaging (computerized virtual domain) can be linked up and registered. In this way, the geometric coordination of the object/imaging can be defined and its orthogonal images would be fixed on defined planes. The images can then be measured with vector information and serial imagings can also be directly compared.**

Keywords: Cone beam computed tomography, Cartesian coordinates, mapping, measurement, rigid registration

I. Introduction

Computed tomography (CT) produces a 3D imaging reconstructed from a serial of 2-dimensional (2D) planar projections using mathematic algorithm [13]. Traditional CT uses a narrow fan-shaped x-ray beam to acquire image slices and that requires multiple rotational sequences. In contrast, CBCT utilizes a radiation beam in cone shape which requires only one rotational sequence to acquire sufficient data for imaging reconstruction. Hence, the acquisition time is reduced and the radiation dose imposed to a patient is significantly lower than CT.

The primary purpose of prescribing CT/CBCT is to "look through" a patient (object) in a non-invasive way. The reconstructed images are usually presented as a 3D imaging of the object in the selected FOV, that is the scan volume of the machine and the anatomical structures captured. FOV in the maxillofacial region can range from full skull, upper jaw and lower jaw, upper jaw only and lower jaw only. Small FOV limiting the area of interest (AOI) only is recommended to reduce the radiation dosage (as low as reasonably practicable ALARP): e.g, International Commission on Radiological Protection (ICRP) 1977. The imaging is a reflection of the radiopacity of the object, which is defined as the ability to obstruct the radiation and therefore reflects the density and architecture of the structure. The radiopacity will be digitalized in a spectrum of grayscale values from black to white with 2^8 (256) shades in 8-bit data or 2^{12} (4096) shades in 12-bit data [5]. To "look through" the object, three cross-sectional 2D images are presented in an orthogonal manner with respect to x-, y- and z- planes (clinically sagittal, coronal and transverse planes) (Fig 1) showing the spatial relationship of structures. These planes are of utmost important in the diagnosis of diseases and planning of treatments.

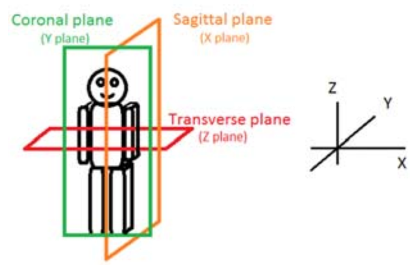

Fig. 1. The sagittal, coronal and transverse planes and the x-. y- and z- axis

The default setting of the transverse view is parallel to the horizontal plane of most CBCT machines which scan the patient in an upright position. Before acquisition, the patient was seated and his/her head was positioned with the help of horizontal and vertical guiding lasers of the machine. It's relatively easy to align patient to the vertical laser to his/her facial midline. Frankfurt horizontal plane (FHP), a horizontal plane of the bony structures from the lower margin of the left orbit (Orbitale) to the upper margins of the ear canals (Poria), may be used to align the patient to the horizontal plane. However, sometimes the resultant orthogonal views might not be the best clinical views and hence clinicians have to orientate the 3D imaging by themselves. For cases in which a small FOV is used, there will be insufficient anatomical landmarks and the clinicians might wrongly orientate the orthogonal views which look similar to the genuine ones. This can lead to geometric errors when analyzing the relationship of structures in these images and cause clinical disaster such as damage of vital structures (Fig 2). Furthermore, it is also extremely difficult to reproduce patient's head position by bony anatomical landmarks which are might be clinically invisible. The loss of an standardized orientation precludes the comparison of serial imagings taken at different time such as measuring the deviation of dental implant position after placement from the planning (Fig. 3(a)).

Walter Y.H. Lam, Peter Y.P. Wat, Henry W.K. Luk and Edmond H.N. Pow, Oral Rehabilitation, Faculty of Dentistry, The University of Hong Kong, Hong Kong S.A.R., China (phone: 852-2859-0305; fax: 852-2858-6114; e-mail: ehnpow@hku.hk).

Henry Y.T. Ngan, Department of Mathematics, Hong Kong Baptist University, Kowloon Tong, Hong Kong S.A.R., China (e-mail: ytngan@hkbu.edu.hk).

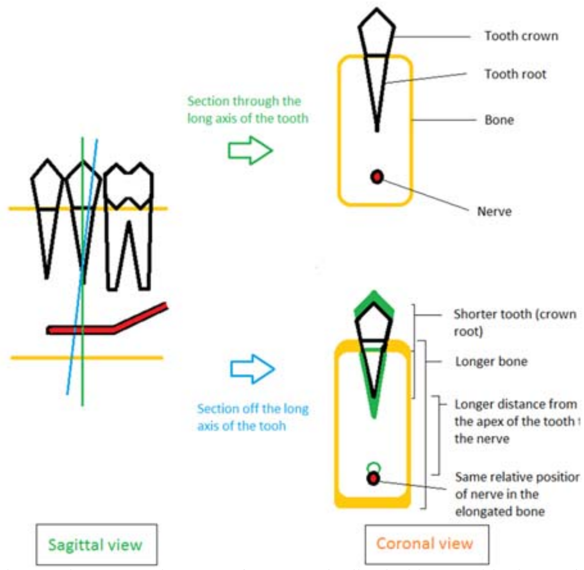

Fig. 2. The geometric error of non-standardized object positioning and resultant cross sectional (coronal) views. The apparent increased safety distance from the apex of tooth to nerve in the "off tooth axis" cut may lead to nerve damage if surgery is done.

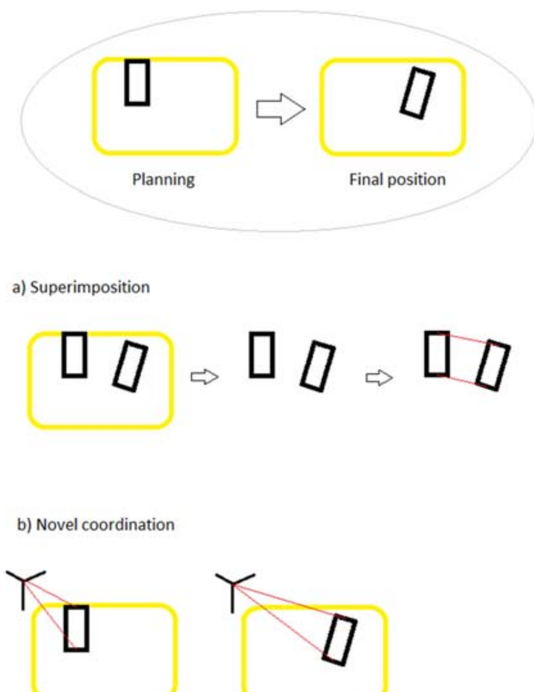

Fig. 3. Comparison of serial imagings: (a) Superimposition; (b) Novel coordination.

Owing to the problems as described, there is a need to develop a novel geometric coordination registration of CBCT imaging based on a standardized reference (fiducial) marker for the clinical measurements. It can potentially eliminate errors when performing a match between the clinical object in the real physical domain and the computerized virtual domain in imaging. This also allows easy comparison between serial computerized virtual domains (Fig 3(b)).

This paper contributes in three-fold areas: (1) To the best of our knowledge, this is the first study to propose a novel and simple geometric coordination registration in the CBCT. This gives an orientation to the 3D imaging and allows a comparison of serial imagings by a simple way; (2) Since the real physical domain (object) and the computerized virtual domain (imaging) share the same coordination system, the virtual planning can easily be transferred to the reality; (3) This physical-virtual linkage may provide an method to determine the validity of various algorithms (feature based or intensity based) used to align and superimpose serial imagings.

The organization of this paper is as follows: Section II outlines the related work. Section III presents the details of the proposed geometric coordination registration. Section IV presents the experimental result. Lastly, conclusion is drawn in Section V.

II. Related Work

Diagnostic imagings, enabling clinicians to "see through" the internal structures of a body without breaching it, are indispensable in the modern minimum invasive medicine. Tomogram involving gather 2D projection data from multiple directions and these data will be processed by a computer in CT [6]. CBCT is a variation of CT which is used to reconstruct 3D structures of the head and neck, for which technology were developed and marketed in 1990s [1]. It is a useful 3D diagnostic tool and various clinical applications including dental implant planning, visualization of abnormal teeth, evaluation of the jaws and face, cleft palate assessment, diagnosis of dental caries (cavities), endodontic (root canal) diagnosis, and diagnosis of oral and maxillofacial trauma has been suggested [15].

Orientation of the 3D imaging and its orthogonal images are important in analyzing the actual spatial relationship of the human body structures (Fig 2). Full skull FOV may be prescribed and the bony landmarks of the skull can be used to orientate the imaging as well as defining Cartesian coordination in the imaging [2, 14], however the FOV of the imaging should be limited to the AOI only to maintain the minimum radiation as well as the potential medico-legal implications against the clinicians for missed pathology in FOV but outside the AOI. On the other hand, a reproducible clinical position, called natural head position (NHP) [16], was suggested to orientate the imaging. This requires specialized equipment with extra steps to determine the NHP and transfer to the imaging.

The lack of standardized orientation of 3D imaging and its orthogonal views precludes simple comparison of serial imagings. The software computes the best fit between imagings by surfaces or landmark points (feature based) or individual voxels (image unit of the imaging) (intensity based) to obtain a transformation matrix for rotation and translation, thereby both images will employ the same coordinate system. The difference was described in a relative manner [4]. This requires specialized software which has not been validated on any proposed superimposition algorithm.

This paper proposes to define Cartesian coordinates in the CBCT imaging (computerized virtual domain) using a corner of a cube with radiopaque painting (real physical domain). The corner tip of the cube represents the Cartesian origin (0_x, 0_y, 0_z), the three edges are the three axes (x-, y- and z- axis) and the three surfaces are the three planes (x-, y- and z- plane) (Fig. 4(a)). The cube may be positioned arbitrary or according to clinical interest (e.g. parallel to FHP or NHP). This allows the clinicians to orientate the imaging with reference to the cube in a small FOV. Each voxel unit of the CBCT imaging would be assigned with a coordinate. This is simple and easily fabricated using parallelometer or prefabricated building brick Lego [7]. The coordination of a specific point can be obtained by simple measurement respective to the axes. The accuracy of linear measurement of CBCTs has been validated in several studies [9, 11]. If the corner of the cube is seated on the same position in the object, this registered coordinates in serial imagings for comparison uses free DICOM viewer software with a linear measurement function (Fig. 4(b)).

(a) Acrylic appliance sitting on the stone model of upper jaw

(b) Corner highlighted by colored lines

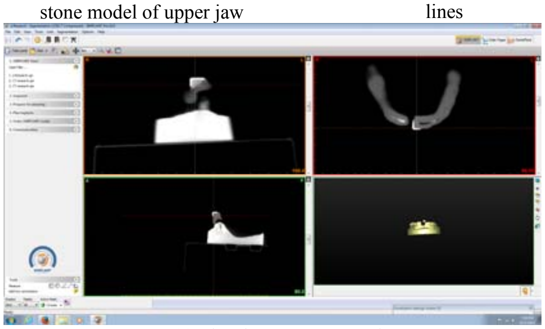

(c) SimPlant Pro screen view

Fig. 4. (a) A clinical example of corner of cube being a part of acrylic appliance sitting on the stone model of upper jaw; (b) corners of cube highlighted by colored lines; (c) SimPlant Pro screen view. Lower right window showing the 3D imaging, Upper right window (red border) showing the transverse view, upper left (orange border) and lower left windows (green border) showing the sagittal view and coronal view respectively.

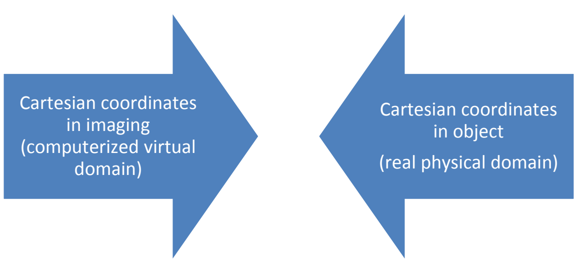

Fig. 5. Mapping with imaging and object.

III. Geometric Coordination Registration

This section presents how a novel geometric coordination registration (Fig. 5) is proposed for the computerized virtual domain and the real physical domain. This is a feature based (using the corner of a cube) rigid (linear) transformation.

A. Cartesian coordinates in the object (real physical domain)

In this conceptual paper, an acrylic cube was used to define the Cartesian coordinates. One corner of the cube was chosen to be the origin (0_x, 0_y, 0_z) and the three orthogonal surfaces forming this corner represent the x-, y- and z- planes. Where two planes intersect, these represent the axis. (Fig. 6)

Definition 1. Mathematically, the (x, y, z)-coordinates of a real object i can be expressed as

$$O_i = (x_i, y_i, z_i). \quad (1)$$

B. Cartesian coordinates in the imaging (computerized virtual domain)

Orthogonal views are x-, y- and z- plane cross-sectional views of a 3D imaging. The window-frames showing these views are color-coded (red, orange and green in the SimPlant Pro software) (Figs. 4(b) and 6). In each orthogonal view, the positions of other two views are shown with dotted lines (named as virtual axes) and same colored as the corresponding window-frame for easy identification. While one orthogonal view is being scrolled, its virtual axis in other two orthogonal views will move accordingly and the clinician will understand the position of cross-section with respect to the 3D imaging.

If the orthogonal views remain static in specific cross sections, the virtual axes will be fixed. The intersection between three virtual axes will become the origin (0_x, 0_y, 0_z) and the virtual axes become the x-, y-, and z-axes, therefore the imaging is defined with Cartesian coordination.

Definition 2. The (x, y, z)-coordinates of the computerized object i can be expressed as

$$C_i = (X_i, Y_i, Z_i). \quad (2)$$

C. Mapping the real physical domain to the computerized virtual domain (Registration)

For the mapping, radiopaque concentrated Barium Sulphate ($BaSO_4$) solution was mixed and painted in thin film on the corner of the cube. During the CBCT acquisition, the corner will appear opaque (whitish grey) in the imaging. By mapping the virtual axes of the imaging to the opaque corner of the cube, the computerized virtual domain was linked up to the real physical domain. A point *a* in the cube will have the same coordinate as the corresponding voxel of the point *a* in the imaging. In this way, measuring the difference between point *a* and point *b* in the imaging will yield the distance as well as the vector information in the physical object in a non-invasive manner (Fig. 7).

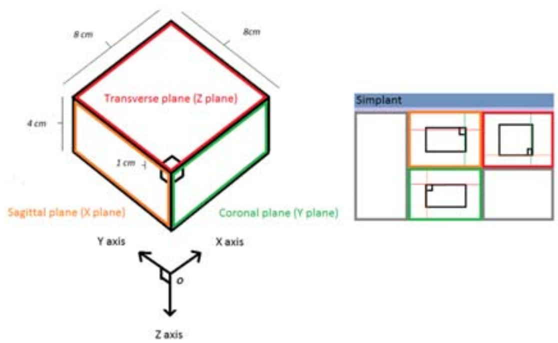

Fig.6. The cube surfaces (physical) and the simplified SimPlant Pro views (virtual).

Definition 3. A simple image registration should be an objective mapping which can be expressed as

$$F(O_i) = C_i \tag{3}$$

for a real object i to the computerized object i in the CBCT.

Definition 4. A rigid registration should be achieved by a measurement of similarity S by a normalized cross correlation (NCC) between two computerized objects C_i^1 and C_i^2 from a real object O_i such that

$$S(C_i^1, C_i^2) = \frac{(C_i^1, C_i^2)_{L^2}}{\|C_i^1\|_{L^2}\|C_i^2\|_{L^2}} \tag{4}$$

This normalized cross correlation should offer a metric of image registration in any two trials to see whether they could generate the closely or the same (x, y, z)-coordinates in the computerized domain. In this paper, a square root of distance between various two computerized objects C_i^1 and C_i^2. The This NCC will be measured in the detailed experiments in future.

C. Experiment

An acrylic cube ($8cm \times 8cm \times 4cm$) in the dimension of human jaw with one of its corner painted with thin layer of $BaSO_4$ and the three surfaces forming this corner was defined as x-, y- and z-plane. The area of the painting was $1cm \times 1cm$ at each of the corner surfaces (Fig. 6). $1mm$ diameter of $BaSO_4$ points were painted on the x-, y- and z- planes and were labeled and protected by adhesive tape.

An experiment to prove our concept was carried out. The cube was deliberately located in a position to map with the virtual axes with minimum rotation of the reconstructed 3D imaging so as to minimize any image distortion and geometric error due to rotation [10]. Horizontally, the cube was placed on the calibrating platform which was provided by the manufacturer for seating the cylindrical hollow tube to calibrate the CBCT machine (iCAT classic 3D imaging system, Imaging Science International Inc., Hatfield, PA, USA). Physically, the horizontal plane of the cube would be in parallel with the horizontal level of the CBCT machine. Virtually, the horizontal orthogonal views of the 3D imaging would be in parallel with the horizontal virtual axis. On the other hand, the vertical position of the cube was guided by the vertical laser guiding beam of the CBCT machine. The vertical and the horizontal laser guiding beams were intended to position the patient in the center of FOV.

A protocol of a scan was selected with the largest FOV and highest available resolution (i.e. full 13 cm 40 seconds 0.25 voxel high resolution). 599 frames of 2D planar images were acquired. The imaging was transferred from the iCAT workstation to a personal computer (Dell Precision T1700 workstation with a graphic card NVIDIA Quadro K2000 and a 23-inch Dell P2314H LED monitor with a screen resolution of 1920 × 1080) loaded with an implant planning software SimPlant Pro (Version 16.0, Materialise NV, Leuven, Belgium) in the format of digital imaging and communications in medicine (DICOM).

This experiment consists of both physical and virtual measurements of 1) the linear distances between points and 2) the coordinate of points, which is the perpendicular linear distance from the x-, y- and z-axes. These were measured from

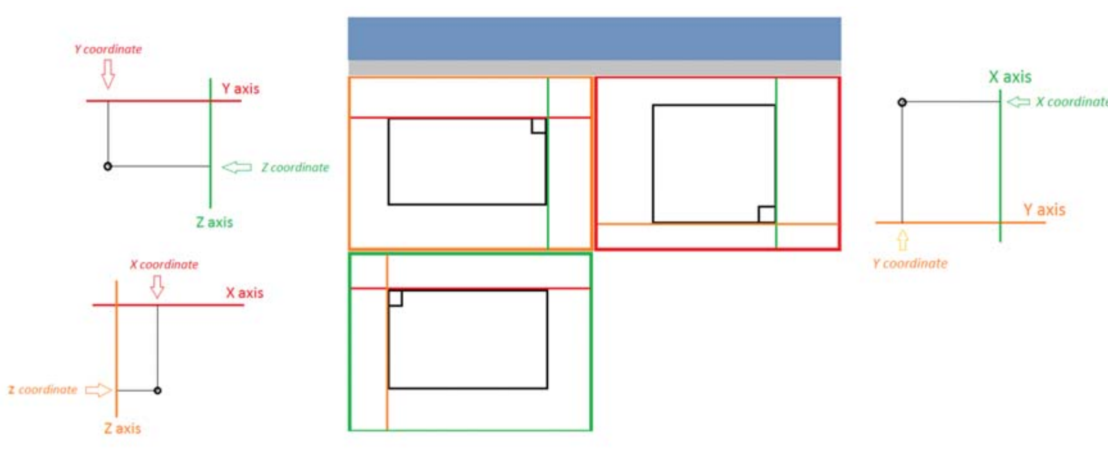

Fig. 7. (x, y, z)-coordination measurement by SimPlant Pro when the virtual axes mapped to reference marker located at the corner of a cube.

(a) 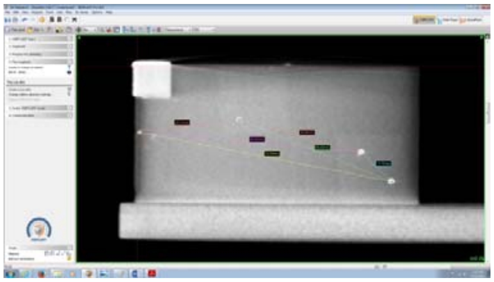

(b) 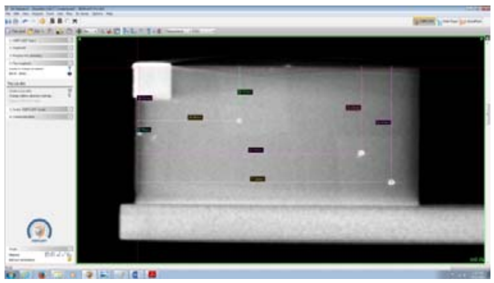

Fig. 8. (a) Measurement of linear distances between points (b) Measurement of coordinate of points by SimPlant Pro (virtual).

the center of points. SimPlant Pro (virtual) measurement was accuracy to 2 decimal places and was performed by one investigator (Fig. 8). The cube was physically measured (gold standard) by a digital toolmakers microscope (accuracy to 0.0025mm) (Leitz Wetzlar WM Standard Toolmarkers' microscope, Germany) by another investigator. The microscope has a movable table (XY stage) which the measuring object located on and allows two axis (x- and y-) movements. To measure distance between point *a* and point *b*, by setting point *a* as the reference measuring point (0_x, 0_y) and moving the XY stage to point *b*, the distance of point *a* to point *b* will be presented in x- and y- component. Distance can then be calculated by$\sqrt{x^2 + y^2}$. Coordinate of points was measured by registration of the reference measuring point of the toolmaker to the corner of the cube (0_x, 0_y, 0_z) and the coordination of that point was obtained directly.

Difference between the physical and the virtual measurement is calculated by subtracting the virtual from physical one. If the result is positive, virtual measurement is underestimated while if the result is negative, virtual measurement is overestimated. Difference between the coordination of a point in the physical and the virtual domain was calculated by$\sqrt{\Delta x^2 + \Delta y^2}$.

IV. Experimental Result

4.1 Results

The mean difference of linear measurement at $x-, y-$ $and\ z-planes$ was $-$ 0.21mm (Median = $-$ 0.20mm, Standard deviation (SD) = 0.16) and this corresponding to almost one voxel size of the imaging (Table 1). The virtual measurement is overestimated. The mean difference of linear measurement of coordinates at $x-, y-\ and\ z-planes$ was 0.55mm (Median = 0.55mm, SD = 0.27). This measurement is underestimated. The mean square root difference of the coordinates at x-, y- and z-planes was 0.83 (Median = 0.87, SD = 0.23) (Table 2).

4.2 Discussion

The linear measurement of CBCT in this study show similar degree of accuracy as the previous studies [9, 11]. This means the CBCT is an accurate diagnostic tool in linear measurement. Errors in identifying the center of a point during measurement have been suggested as a major source of measuring error. The difference in the coordinate measurement in this study is below 1mm and this is in agreement with Lagravere's study [8] in which 3D x-, y- and z- coordinate measurement was performed. Their single axis error ranges from 0.53mm to 0.75mm. It was anticipated that 3D measurements are less accurate than linear measurement since any errors in linear measurement are accumulated in 3D.

It is interesting to discover: when we measure the linear distance between two points and the virtual SimPlant Pro measurements are larger than the physical one, this is regarded as an over-estimation. Conversely, when we measure the linear distance between a point and axis (coordinate) and the virtual SimPlant Pro measurements become smaller, this is an under-estimation. Both over- and under-estimation of measurements in one imaging were reported [3, 12] without explanation, further studies are needed to clarify this issue.

The proposed novel geometric coordination registration successfully mapped the real physical domain to the computerized virtual domain. The accuracy of this registration process depends on the accuracy of 1) the measurement of perpendicular linear distances from the x-, y-, and z-axes (i.e. coordinates), 2) the mapping procedure [17]. In Lagravere's study, the imaging coordination was automatically defined by software based on anatomical markers. In contrast, the virtual x-, y- and z- axes (i.e. coordinate) were defined manually in this study and may be less accurate. Therefore, the proposed novel geometric coordination may yield a more accurate result if the mapping procedure can be performed automatically by software.

Its application in the comparison of serial imagings depends on the reproducibility of the reference (fluicidal) markers in the object. Bone and teeth are hard tissues that are relatively stable anatomical structure in the head and neck regions. Teeth are easily reached while bone is usually covered with soft tissues. Acrylic stent with the incorporation of $BaSO_4$ painted corner can rest on the upper/lower teeth and that should be stable for a reasonable period of time (Fig. 4 (a)). The mapping between the physical and virtual domain may provide a method to validate the accuracy of various superimposition algorithms. Moreover, accurate transfer of the computerized surgical planning to reality is possible including dental implant placement, radiotherapy and robotic surgery.

Diagnostic value of the CBCT imagings extends to the fabrication of stereolithographic (SLG) models. Based on the 3D imaging, a 3D physical model can be made by additive (printing) or subtractive (milling) methods. Clinician can perform model surgery on these SLG models. The mapping between the computerized virtual domain and the real physical domains is therefore a two-way approach and enables for a validation of the accuracy of SLG models and the original scanned object.

TABLE I.
THE LINEAR MEASUREMENT RESULT.

Linear Distance (in mm)	Microscopy measurement	SimPlant measurement	Difference i.e. Microscopy – Simplant
Plane X (4 points)			
Point 1 to point 2	28.14	28.11	0.03
Point 1 to point 3	62.42	62.62	-0.20
Point 1 to point 4	71.66	72.04	-0.38
Point 2 to point 3	35.52	35.69	-0.17
Point 2 to point 4	45.87	46.22	-0.35
Point 3 to point 4	11.51	11.75	-0.24
Plane Y (3 points)			
Point 1 to point 2	34.67	34.75	-0.08
Point 1 to point 3	58.74	59.03	-0.29
Point 2 to point 3	24.64	24.93	-0.29
Plane Z (7 points)			
Point 1 to point 2	70.22	70.65	-0.43
Point 1 to point 3	53.12	53.46	-0.34
Point 1 to point 4	54.59	54.96	-0.37
Point 1 to point 5	58.45	58.93	-0.48
Point 1 to point 5	38.19	38.32	-0.13
Point 1 to point 6	18.66	19.09	-0.43
Point 1 to point 7	24.73	24.91	-0.18
Point 2 to point 3	16.16	16.10	0.06
Point 2 to point 4	17.92	18.02	-0.10
Point 2 to point 5	49.07	49.11	-0.04
Point 2 to point 6	53.49	53.44	0.05
Point 3 to point 4	12.45	12.60	-0.15
Point 3 to point 5	28.36	28.76	-0.40
Point 3 to point 6	46.76	47.06	-0.30
Point 3 to point 7	40.50	40.70	-0.20
Point 4 to point 5	15.96	16.27	-0.31
Point 4 to point 6	39.05	39.25	-0.20
Point 4 to point 7	38.75	38.83	-0.08
Point 5 to point 6	31.76	31.86	-0.10
Point 5 to point 7	40.24	40.37	-0.13
Point 6 to point 7	21.53	21.47	0.06

Table II.
THE COORDINATE MEASUREMENT RESULT

	Distance to X-axis	Distance to Y-axis	Distance to Z axis	SRD
Plane X				
Point 1	0	1.49/0.79/0.70	19.53/18.55/0.98	1.20
Point 2	0	29.42/28.65/0.77	15.42/15.27/0.20	0.80
Point 3	0	63.83/62.94/0.89	24.44/24.26/0.18	0.91
Point 4	0	72.01/71.42/0.59	32.42/32.47/-0.05	0.59
Plane Y				
Point 1	62.71/62.09/0.62	0	0.80/0.00/0.80	1.01
Point 2	36.87/36.33/0.54	0	24.13/23.40/0.73	0.91
Point 3	14.55/13.81/0.74	0	34.61/34.10/0.51	0.90
Plane Z				
Point 1	1.44/0.96/0.48	42.98/42.32/0.66	0	0.82
Point 2	71.37/70.94/0.43	36.52/35.73/0.79	0	0.90
Point 3	50.66/50.34/0.32	23.11/22.04/1.07	0	1.12
Point 4	55.39/54.98/0.41	34.57/33.80/0.77	0	0.87
Point 5	59.40/59.28/0.12	49.93/49.60/0.33	0	0.35
Point 6	31.93/31.57/0.36	65.88/65.32/0.56	0	0.67
Point 7	19.16/18.85/ 0.31	48.55/48.02/0.53	0	0.61

Remark: Distance to X-, Y-, Z-axes [Microscopy/SimPlant/Difference], Square root of distances (SRD)

V. CONCLUSIONS

This paper proposes a novel registration method for CBCT between the object (real physical domain) and imaging (computerized virtual domain). The corner of the cube may be defined arbitrarily or by a clinical significance. With a reference to the cube corner, even with a limited FOV, the clinician can have an orientation of the imaging which is critical in analyzing the relationship between structures. After the registration under the same Cartesian coordinate mapping, serial imagings can be monitored using free viewer softwares that can measure distances between two points. Potential clinical applications were also discussed.

REFERENCES

[1] Y. Arai, E. Tammisalo, K. Iwai, K. Hashimoto, K. Shinoda, "Development of a Compact Computed Tomographic Apparatus for Dental Use," *Dentomaxillofac Radiol.*, 28(4), pp.245-248, 1999.

[2] A. DeCesare, M. Secanell, MO. Lagravère, J. Carey, "Multiobjective Optimization Framework for Landmark Measurement Error Correction in Three-dimensional Cephalometric Tomography," *Dentomaxillofac Radiol,* vol. 42, no. 7, 20130035, 2013.

[3] R.A. Fuhrmann, A. Bucker, P.R. Diedrich, "Assessment of Alveolar Bone Loss with High Resolution Computed Yomography," *J Periodontal Res.,* vol. 30, no. 4, pp. 258-263, 1995.

[4] D. Grauer, L.S. Cevidane, M.A. Styner, J.L. Ackerman, W.R. Proffit, "Pharyngeal Airway Volume and Shape from Cone-beam Computed Tomography: Relationship to Facial Morphology," *Am. J. Orthod. Dentofacial Orthop.* vol. 136, no. 6, pp.805-814, 2009.

[5] D.C. Hatcher, C.L. Aboudara, "Diagnosis Goes Digital," *Am. J. Orthod. Dentofacial Orthop.,* vol. 125, no. 4, pp. 512-515, 2004.

[6] G.T. Herman, Fundamentals of Computerized Iomography: Image Reconstruction from Projection, 2nd edition, *Springer*, 2009.

[7] S. Holst, M.B. Blatz, S. Eitner, "Precision for Computer-guided Implant Placement: using 3D Planning Software and Fixed Intraoral reference points," *J. Oral Maxillofac. Surg.,* 65(3), pp. 393-399, 2007.

[8] M.O. Lagravère, J. Carey, R.W. Toogood, P.W. Major, "Three-dimensional Accuracy of Measurements Made with Software on Cone-beam Computed Tomography Images," *Am. J. Orthod. Dentofacial Orthop.,* vol. 134, no. 1, pp. 112-116, 2008.

[9] C.A. Lascala, J. Panella, M.M. Marques, "Analysis of the Accuracy of Linear Measurements obtained by cone beam computed tomography (CBCT-NewTom),", vol. 33, no. 5, pp.291-294, 2004.

[10] H. Lund, K. Gröndahl, H.G. Gröndahl, "Accuracy and Precision of Linear Measurements in Cone Beam Computed Tomography Accuitomo Tomograms Obtained with Different Reconstruction Techniques," *Dentomaxillofac. Radiol.,* 38(6), pp. 379-386, 2009.

[11] H.M. Pinsky, S. Dyda, R.W. Pinsky, K.A. Misch, D.P. Sarment, "Accuracy of Three-dimensional Measurements using Cone-beam CT," *Dentomaxillofac. Radiol.*, vol. 35, no. 6, pp.410-416, 2006.

[12] T. Razavi, R.M. Palmer, J. Davies, R. Wilson, P.J. Palmer, "Accuracy of Measuring the Cortical Bone Thickness Adjacent to Dental Implants using Cone Beam Computed Tomography," *Clin. Oral Implants Res.*, vol. 21, no. 7, pp. 718-725, 2010.

[13] W.C. Scarfe, A.G. Farman, "What is Cone-beam CT and How Does It Work?," *Dent. Clin. North Am.,* vol. 52, no. 4, pp. 707-730, 2008.

[14] G.R. Swennen, F. Schutyser, E.L. Barth, P. De Groeve, A. De Mey, "A New Method of 3-D Cephalometry Part I: the Anatomic Cartesian 3-D Reference System," *J. Craniofac. Surg.*,12(2), pp. 314-325, 2006.

[15] [online] United State Food and Drug Administration, Dental Cone-beam Computed Tomography, http://www.fda.gov/Radiation-EmittingProducts/RadiationEmittingProductsandProcedures/MedicalImaging/MedicalX-Rays/ucm315011.htm, 2014.

[16] J.J. Xia, J.K. McGrory, J. Gateno, J.F. Teichgraeber, B.C. Dawson, K.A. Kennedy, R.E. Lasky, J.D. English, C.H. Kau, K.R. McGrory, "A New Method to Orient 3-dimensional Computed Tomography Models to the Natural Head Position: a Clinical Feasibility Study," *J. Oral Maxillofac. Surg.,* vol. 69, no.3, pp. 584-591, 2011.

[17] X.C. He and N.H.C. Yung, "New Method for Overcoming ill-conditioning in Vanishing-point-based Camera Calibration," *Opt. Eng.*, 46(3), 037202, 2007.